The Journal of Chemical Physics ARTICLE scitation.org/journal/jcp

Numerical tests of coherence-corrected surface hopping methods using a donor-bridge-acceptor model system

Cite as: J. Chem. Phys. 150, 194104 (2019); doi: 10.1063/1.5092999
Submitted: 15 February 2019 • Accepted: 25 April 2019 •
Published Online: 16 May 2019

Andrew E. Sifain,[1,2] Linjun Wang,[3] Sergei Tretiak,[2,4] and Oleg V. Prezhdo[1,5,a)]

AFFILIATIONS

[1]Department of Physics and Astronomy, University of Southern California, Los Angeles, California 90089-0485, USA
[2]Theoretical Division, Center for Nonlinear Studies and Center for Integrated Nanotechnologies, Los Alamos National Laboratory, Los Angeles, New Mexico 87545, USA
[3]Center for Chemistry of Novel and High-Performance Materials and Department of Chemistry, Zhejiang University, Hangzhou 310027, China
[4]Skolkovo Institute of Science and Technology, Moscow 143026, Russia
[5]Department of Chemistry, University of Southern California, Los Angeles, California 90089-1062, USA

[a)]**Electronic mail:** prezhdo@usc.edu

ABSTRACT

Surface hopping (SH) is a popular mixed quantum-classical method for modeling nonadiabatic excited state processes in molecules and condensed phase materials. The method is simple, efficient, and easy to implement, but the use of classical and independent nuclear trajectories introduces an overcoherence in the electronic density matrix which, if ignored, often leads to spurious results, such as overestimated reaction rates. Several methods have been proposed to incorporate decoherence into SH simulations, but a lack of insightful benchmarks makes their relative accuracy unknown. Herein, we run numerical simulations of common coherence-corrected SH methods including Truhlar's decay-of-mixing (DOM) and Subotnik's augmented SH using a Donor-bridge-Acceptor (DbA) model system. Numerical simulations are carried out in the superexchange regime, where charge transfer proceeds from a donor to an acceptor as a result of donor-bridge and bridge-acceptor couplings. The computed donor-to-acceptor reaction rates are compared to the reference Marcus theory results. For the DbA model under consideration, augmented SH recovers Marcus theory with quantitative accuracy, whereas DOM is only qualitatively accurate depending on whether predefined parameters in the decoherence rate are chosen wisely. We propose a general method for parameterizing the decoherence rate in the DOM method, which improves the method's reaction rates and presumably increases its transferability. Overall, the decoherence method of choice must be chosen with great care and this work provides insight using an exactly solvable model.

I. INTRODUCTION

Surface hopping (SH)[1] is a mixed quantum-classical method that is used for modeling nonadiabatic excited state processes in molecules and condensed-phase materials.[2–10] Its underlying approximation is the representation of a nuclear wavepacket as a swarm of independent and classical nuclear trajectories. The method's popularity is leveraged by its efficiency and ease of implementation, but the classical description of nuclei introduces well-known setbacks including lack of nuclear tunneling, lack of zero-point energy, and overcoherence. Decoherence is the process by which nuclear wavepackets on different potential energy surfaces decouple and move independently. In surface hopping, the electronic wavefunction is integrated coherently along every (independent) trajectory, resulting in an overcoherence between electronic states.[11] Long-time dynamics[12] and systems with several regions of nonadiabatic coupling[13] are susceptible to spurious results without the inclusion of decoherence. From the perspective of excited state

relaxation, decoherence is particularly important when wavepacket separation is faster than the time needed to stabilize a coherent electronic transition; this depends on the electronic manifold in which relaxation occurs. For systems with a quasicontinuum of electronic states, decoherence may not be so important as a high density of states facilitates fast electronic transitions.[14,15] By contrast, well-separated energy levels and localized states result in much slower relaxation. This effect is seen for the electron-hole recombination across the bandgap in quantum-confined materials such as quantum-dots and carbon nanotubes.[16,17] Neglecting decoherence in these materials leads to underestimating dephasing time scales by several orders of magnitude.

There are a number of proposed methods that incorporate decoherence into surface hopping simulations.[18–26] The vast majority can be boiled down to defining a decay rate indicative of wavepacket separation. Yet even a simple collapse approach of the electronic wavefunction has been applied to calculate transition rates in a spin-boson model, which has proven successful in recovering the correct quadratic-scaling in diabatic coupling.[27] The decoherence time scale has also been estimated using a Gaussian wavepacket approximation with width given by the thermal de Broglie wavelength.[24–26,28] A more mathematically driven method is Augmented Fewest-Switches Surface Hopping (FSSH) (A-FSSH), which involves a moment expansion of the Liouville equation that gives rise to time-dependent uncertainties in nuclear position and momentum.[21] These uncertainties are propagated along the nuclear trajectory and are variables of the collapse rate. A-FSSH recovers Marcus theory[29,30] and improves branching ratios in model systems.[13,21] A recent study using a spin-boson model has also found that A-FSSH improves results compared to exact calculations over a wide range of energetic and coupling parameters.[31] Here, we would like to benchmark the most popular decoherence methods by calculating their nonadiabatic charge transfer rates in a Donor-bridge-Acceptor (DbA) model system whose standard reaction rates are obtainable using Marcus theory.

In DbA-type systems, charge transfer from a donor to an acceptor proceeds through intermediate states called bridges.[32] When the energy gap between the donor and bridge is large relative to the thermal energy, superexchange theory predicts a tunneling mechanism for charge transfer.[33–35] Experimental studies have described electronic tunneling through DNA hairpins[36,37] and oligo-*p*-xylene bridges.[38,39] In such studies, the effect of the tunneling energy gap is probed by measuring the rate of charge transfer from a donor to an acceptor as a function of the number of bridging units. The charge transfer rate exponentially decays as a function of distance,[40] and the distance decay constant can be related to an expression for tunneling through a finite barrier to estimate an effective tunneling energy gap.[41–43] Not surprisingly, experimental evidence shows that the outcome and efficiency of the tunneling mechanism is related to the size of the gap. As more DbA systems are predicted, synthesized, and ultimately used for applications,[44,45] it is important that the tools of excited state modeling (e.g., surface hopping) correctly describe the superexchange mechanism for charge transfer.

In this paper, global flux surface hopping (GFSH)[46,47] is combined with the following popular decoherence corrections: Truhlar's decay-of-mixing (DOM)[48] and Subotnik's augmented surface hopping.[21] Donor-to-acceptor reaction rates are compared to the rates computed using Marcus theory.[49] This work investigates the surface hopping description of superexchange for charge transfer and adds to the body of literature[31,50–53] aimed at assessing the reliability of and improving the surface hopping method for nonadiabatic molecular dynamics. The paper is organized as follows: Sec. II reviews the overcoherence problem of surface hopping, Sec. III describes superexchange theory and the superexchange reaction rate given by Marcus theory, and Sec. IV describes the tested decoherence methods and simulation details, including the DbA model used for benchmarking. Finally, results of the simulations and conclusions are provided in Secs. V and VI, respectively.

II. OVERCOHERENCE PROBLEM OF SURFACE HOPPING

In exact dynamics, the total wavefunction $|\psi\rangle$ can be represented in terms of coupled electronic and nuclear wavefunctions through the Born-Oppenheimer expansion[54]

$$|\psi\rangle = \sum_i |\chi_i\rangle|\phi_i\rangle, \tag{1}$$

where $|\phi_i\rangle$ are adiabatic electronic states determined at fixed nuclear geometries and $|\chi_i\rangle$ are nuclear states. The electronic density matrix (σ) is determined by tracing the combined nuclear-electronic density matrix ($|\psi\rangle\langle\psi|$) over the nuclear degrees of freedom ($\mathbf{R}$)[55]

$$\begin{aligned}\sigma &= \sum_i \sum_j \int d\mathbf{R} \langle\chi_j|\mathbf{R}\rangle\langle\mathbf{R}|\chi_i\rangle|\phi_i\rangle\langle\phi_j| \\ &= \sum_i \sum_j \langle\chi_i|\chi_j\rangle|\phi_i\rangle\langle\phi_j|.\end{aligned} \tag{2}$$

Equation (2) shows that elements of σ depend on the overlap of nuclear wavepackets. In the adiabatic representation, diagonal elements of σ are adiabatic state populations and off diagonal elements are coherences. Decoherence is related to the reduction of overlap between nuclear wavepackets on different surfaces, i.e., $\langle\chi_i|\chi_j\rangle \to 0$ for $i \neq j$.

In Surface Hopping (SH), the initially prepared nuclear wavepacket is represented by a swarm of independent and classical trajectories. Each trajectory evolves and stochastically hops between potential energy surfaces according to a hopping algorithm.[1,46] The hopping algorithm depends on the adiabatic state coefficients (c_i) that make up the state

$$|\psi\rangle = \sum_i c_i|\phi_i\rangle. \tag{3}$$

The electronic density matrix in surface hopping (σ^{SH}) takes the form

$$\sigma^{\mathrm{SH}} = \sum_i \sum_j c_i c_j^* |\phi_i\rangle\langle\phi_j|. \tag{4}$$

Equation (4) makes it clear that decoherence must be explicit in the equation of motion of σ, but the electronic Schrödinger equation (with classical nuclear positions treated as parameters) does not have a decoherent term [see the density matrix formulation in Eq. (10) below]. Thus, in order to recover exact quantum mechanics,

surface hopping simulations must be supplemented with a decoherence correction.

A play-by-play of coherence-corrected surface hopping is as follows: A trajectory enters an interaction region, and as a result, there is an exchange of quantum amplitude, c_i, between the interacting states. In this process, the trajectory stochastically hops between the surfaces and continues doing so until it is outside of the interaction region. On account of overcoherence in surface hopping, even when the trajectory is sufficiently far away from the interaction region, there is still nonzero quantum amplitude associated with states that were previously involved in the interaction but that are not currently occupied by the trajectory. Instead, the population of the occupied electronic state ($|\phi_i\rangle$) should approach unity ($c_i = 1$) at a rate known as the decoherence rate. The rate (τ_{ij}^{-1}) at which the occupied electronic state decoheres from all other states ($|\phi_j\rangle$) is the rate at which the overlap of nuclear wavepackets on different potential energy surfaces decays to zero [$\langle\chi_i|\chi_j\rangle \xrightarrow{\tau_{ij}^{-1}} 0$ in Eq. (2)].

III. SUPEREXCHANGE THEORY AND REACTION RATES IN DONOR-BRIDGE-ACCEPTOR SYSTEMS

Previous studies have benchmarked surface hopping and decoherence methods using exactly solvable scattering models such as those originally studied by Tully.[1,13,21,46] In this work, we focus on reaction rates using a DbA model that highlights an electronic tunneling mechanism ubiquitous in many materials.[32] The Hamiltonian of a DbA model with N bridges is $(N+2)\times(N+2)$ and can be written as

$$H = \begin{pmatrix} E_{DD} & V_{Db} & & & & & & & \\ V_{bD} & E_{bb} & V_{bb} & & & & & & \\ & V_{bb} & E_{bb} & V_{bb} & & & & & \\ & & V_{bb} & \dots & & & & & \\ & & & & \dots & V_{bb} & & & \\ & & & & V_{bb} & E_{bb} & V_{bb} & & \\ & & & & & V_{bb} & E_{bb} & V_{bA} & \\ & & & & & & V_{Ab} & E_{AA} \end{pmatrix}. \quad (5)$$

Here, the diagonal and off diagonal elements are diabatic energies and couplings, respectively. The donor and acceptor states are not explicitly coupled, i.e., $V_{DA} = V_{AD} = 0$, but electron transfer proceeds through intermediates. To convey the main pathways, we refer readers to Fig. 1 showing the Liouville space pathways of the density matrix for a three-level system in the *diabatic* representation.[34,56,57] Pathway A of Fig. 1 shows the superexchange pathway, with electron transfer proceeding through coherences without populating bridge state $|2\rangle$. Pathways B and C of Fig. 1 that pass through state $|2\rangle$'s population are referred to as sequential pathways. Superexchange plays the dominant role for electron transfer when bridge states are energetically displaced from the donor and acceptor states (i.e., when bridge states are above the donor and acceptor states by an energy gap that is greater than $k_B T$).

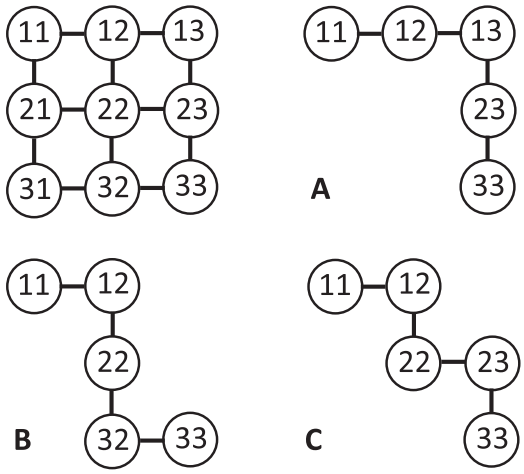

FIG. 1. Liouville pathways from the donor to the acceptor in the diabatic representation. Pathway A is that of superexchange, whereas pathways B and C are sequential pathways that pass through the population of bridge state $|2\rangle$.

The Marcus theory of electron transfer is the seminal work that explains reaction rates from a donor to acceptor chemical species.[49] In order to obtain the Marcus reaction rate during superexchange, the indirect coupling between donor-to-acceptor must be known. In the two-state limit, the energy gap between the surfaces at the crossing is $2V$, where V is diabatic coupling. McConnell derived the energies of the two lowest symmetric and asymmetric eigenstates corresponding to the donor and acceptor states, respectively.[35] McConnell's model assumed an aromatic free radical composed of two phenyl groups, linked together by a series of N methylene groups. In the limit of $|V_{bb}/\Delta\epsilon| \ll 1$, the first-order energy gap, g, is given by

$$g = -\frac{2V_{Db}^2}{\Delta\epsilon}\left(\frac{V_{bb}}{\Delta\epsilon}\right)^{N-1}, \quad (6)$$

where $V_{Db} = V_{bA}$ and $\Delta\epsilon$ is the energy required to remove an electron from the donor or acceptor orbital and place it in a noninteracting bridge orbital. We will refer to $\Delta\epsilon$ as the tunneling energy gap. By deriving the energy gap between a donor and an acceptor, the $(N+2)\times(N+2)$ Hamiltonian reduces to an effective 2×2 Hamiltonian, with direct coupling between a donor and an acceptor given by $g/2$. In the presence of a classical bath, the high-temperature limit reaction rate follows from Marcus theory

$$k_{ET} = \frac{2\pi}{\hbar}\sqrt{\frac{1}{4\pi\lambda k_B T}}\frac{g^2}{4}\exp\left(\frac{-(\lambda-\epsilon_0)^2}{4\lambda k_B T}\right), \quad (7)$$

where λ is the reorganization energy and ϵ_0 is the driving force. Besides the inverted regime and maximum when $\epsilon_0 = \lambda$, the rate scales as $(\Delta\epsilon)^{-2N}$. Equation (7) is a product of a number of approximations including the high-temperature limit and dynamics at thermal equilibrium. The high-temperature approximation is analogous to taking the classical limit. Similarly, surface hopping assumes classical nuclei and thus the Marcus rate serves as a decent reference solution for charge transfer in the DbA model.

IV. METHODS AND SIMULATION DETAILS

We describe GFSH in Sec. IV A,[58] tested decoherence corrections in Sec. IV B, and simulation details in Sec. IV C.

A. Global flux surface hopping

Within GFSH,[46,47] the change of adiabatic state population ($\Delta\sigma_{ii}$) is calculated at each time step as

$$\Delta\sigma_{ii} = \sigma_{ii}(t+\Delta t) - \sigma_{ii}(t). \tag{8}$$

All states are classified into one of the two groups: one with $\Delta\sigma_{ii} < 0$ (group A) and another with $\Delta\sigma_{ii} > 0$ (group B). Transitions can only occur from group A to group B, preserving the minimization criterion of Fewest-Switches Surface Hopping (FSSH).[1] The probability of hopping between the surfaces corresponding to states $|\phi_i\rangle$ and $|\phi_j\rangle$ is given by

$$g_{ij} = \frac{\Delta\sigma_{jj}}{\sigma_{ii}} \frac{\Delta\sigma_{ii}}{\sum_{k\in A}\Delta\sigma_{kk}}. \tag{9}$$

The increase in the population of the target state $|\phi_j\rangle$, $\Delta\sigma_{jj}$, may be attributed to all states assigned to group A. We reduce this quantity to roughly state $|\phi_i\rangle$'s contribution by multiplying $\Delta\sigma_{jj}$ with the change in state $|\phi_i\rangle$'s population relative to the total change in the population of group A, $\Delta\sigma_{ii}/\sum_{k\in A}\Delta\sigma_{kk}$. Finally, the expression in Eq. (9) is divided by the probability of the current state, σ_{ii}, to represent population flux, similar to FSSH. Scattering results comparing GFSH and exact quantum mechanics are provided in the supplementary material. GFSH combined with the augmented decoherence method will be referred to as A-GFSH.

B. Surface hopping dynamics and decoherence corrections

In surface hopping, nuclear trajectories evolve piecewise on adiabatic potential energy surfaces. The electronic density matrix (σ) is integrated with the Liouville-von Neumann equation[1]

$$\dot{\sigma} \approx -\frac{i}{\hbar}\left[E\left(\mathbf{R}^{\mathrm{SH}}\right) - i\hbar\mathbf{d}\cdot\dot{\mathbf{R}}^{\mathrm{SH}}, \sigma\right], \tag{10}$$

where $E\left(\mathbf{R}^{\mathrm{SH}}\right)$ is a diagonal matrix with elements being potential energy surfaces calculated at fixed nuclear geometries ($\mathbf{R}^{\mathrm{SH}}$), $\dot{\mathbf{R}}^{\mathrm{SH}}$ is the velocity of the nuclear trajectory, and $\mathbf{d}$ is the nonadiabatic coupling matrix. Electronic transitions between surfaces occur according to the GFSH algorithm given by Eq. (9). Following a successful hop, the velocity is rescaled along the direction of nonadiabatic coupling. Transitions that are directed upward in energy are rejected if the dispensable kinetic energy does not exceed the energy barrier (also known as frustrated hops). We choose to reverse the nuclear velocity following frustrated hops. In model systems, in which nuclear dynamics are coupled to an implicit bath, reversing the nuclear velocity after frustrated hops leads to reaction rates that are in good agreement with Marcus theory[59] and thermal populations that are in good agreement with the Boltzmann populations.[60]

1. Truhlar's decay-of-mixing

The electronic density matrix is integrated with coherent (c) and decoherent (d) contributions[48]

$$\dot{\sigma} = \dot{\sigma}_{\mathrm{coherent}} + \dot{\sigma}_{\mathrm{decoherent}}. \tag{11}$$

The first term is computed with Eq. (10). The form of the second term is derived from several assumptions such as the electronic state population σ_{kk} for $k \neq K$ (where K is the current state) decays to zero at a rate of $1/\tau_{kK}$, i.e.,

$$\dot{\sigma}^d_{kk} = -\frac{\sigma_{kk}}{\tau_{kK}} \quad (k \neq K). \tag{12}$$

The other conditions used to obtain the time-domain equations for all elements of σ^d are conservation of electronic population, $\sum_k \dot{\sigma}_{kk} = 0$, and conservation of phase angle (θ) in $c_k = |c_k|\exp(i\theta)$. Reference 61 provides a detailed derivation and the explicit form of σ^d.

The expression for the decoherence rate is given by[62]

$$\tau_{ij}^{-1} \sim \frac{|E_i - E_j|}{\hbar}\left(\frac{2mE_0}{\left(\mathbf{P}^{\mathrm{SH}}\cdot\hat{d}_{ij}\right)^2} + C\right)^{-1}, \tag{13}$$

where $\mathbf{P}^{\mathrm{SH}}\cdot\hat{d}_{ij}$ is the nuclear momentum in the direction of nonadiabatic coupling and $C = 1$ and $E_0 = 0.1$ a.u. (atomic units) are empirical parameters chosen based on numerical testing.[62] Equation (13) is an *ad hoc* expression that assumes decoherence does not occur if the momentum in the direction of nonadiabatic coupling is insufficient to support energy transfer [i.e., $\tau_{ij}^{-1} \sim \left(\mathbf{P}^{\mathrm{SH}}\cdot\hat{d}_{ij}\right)^2/2m$ when $\mathbf{P}^{\mathrm{SH}}\cdot\hat{d}_{ij} \to 0$]. Additionally, the decoherence time must be greater than or equal to the shortest electronic time (i.e., $\tau_{ij}^{-1} \leq |E_i - E_j|/\hbar$).[63]

2. Decay-of-mixing dephasing-informed

A drawback of the original decay-of-mixing method (Sec. IV B 1) is a decoherence rate that depends on predefined parameters. Unfortunately, this may limit the method's transferability to systems that differ from those used for fitting. Here, we show a plausible improvement of decay-of-mixing that may overcome this problem. On the basis of Eq. (13), the general form of the decoherence rate is

$$\tau_{ij}^{-1} \sim \alpha|E_i - E_j|, \tag{14}$$

where α is an unknown parameter. Equation (14) eliminates explicit dependence on the kinetic energy [Eq. (13)] for simplicity. We propose an ensemble averaged α, $\alpha \sim \langle\tau_{ij}^{-1}\rangle/\langle|E_i - E_j|\rangle$, where $\langle\ldots\rangle$ denotes statistical mechanical averaging. The ensemble averaged decoherence rate, $\langle\tau_{ij}^{-1}\rangle$, can be estimated by the decay rate of the pure-dephasing function[64]

$$D_{ij}(t) = \exp(-g_{ij}(t)), \tag{15a}$$

$$g_{ij}(t) = \int_0^t \mathrm{d}\tau_2 \int_0^{\tau_2} \mathrm{d}\tau_1 R_{ij}(\tau_1 - \tau_2), \tag{15b}$$

$$R_{ij}(t) = \frac{1}{\hbar^2}\langle\delta\Delta E_{ij}(t)\delta\Delta E_{ij}(0)\rangle, \tag{15c}$$

$$\delta\Delta E_{ij} = E_j - E_i - (\langle E_j\rangle - \langle E_i\rangle), \tag{15d}$$

where $g_{ij}(t)$ is approximated up to second order in the cumulant expansion and $R_{ij}(t)$ is the autocorrelation function of the energy gap fluctuation ($\delta\Delta E_{ij}$). Quantum correlation functions are generally complex, but in the present case, classical molecular dynamics is being used to sample the real part of the autocorrelation function that enters the semiclassical expression for the pure-dephasing function of optical response theory.[65] The optical response pure-dephasing function has been used in many applications of nonadiabatic dynamics.[66–69]

We sample potential energy surfaces while the trajectory evolves in the ground state[70] and do so for a sufficient amount of time so that thermal equilibrium behavior is realized. Although the use of classical path approximation (CPA) to compute α is not necessary for the relatively simple DbA model of the present study, we choose to use this method as it is widely used for dynamics in condensed matter systems.[71] Given adiabatic state energies as a function of time, the dephasing function between any two adiabatic states and their decay rate (determined by fitting the dephasing function to a Gaussian[72]) as well as average gap, $\langle|E_i - E_j|\rangle$, are computed to estimate α. An important physical principle obeyed by this method, which is violated by the out-of-box decay-of-mixing [Eq. (13)], is that wavepackets on parallel surfaces do not decohere: $D_{ij}(t) = 1$ because $R_{ij}(t) = 0$ and consequently $g_{ij}(t) = 0$. Further details clarifying this point can be found in Sec. IV B 3 and Ref. 11.

3. Subotnik's augmented surface hopping

Subotnik's augmented surface hopping is a stochastic collapse approach. The collapse rate depends on dynamic variables of the system including first-order uncertainties (or moments) in nuclear position and momentum.[21] The decoherence rate between the occupied adiabatic state, $|\phi_i\rangle$, and all other states, $|\phi_j\rangle$, is given by

$$\tau_{ij}^{-1} \sim \frac{1}{2\hbar}(\mathbf{F}_{jj} - \mathbf{F}_{ii}) \cdot \delta\mathbf{R}_{jj} - \frac{2}{\hbar}|\mathbf{F}_{ij} \cdot \delta\mathbf{R}_{jj}|, \tag{16}$$

where $\mathbf{F} = -\nabla V|_{\mathbf{R}^{\mathrm{SH}}}$ is the force evaluated at the position of the surface hopping (SH) trajectory and $\delta\mathbf{R} = \mathrm{Tr}_N\{(\mathbf{R} - \mathbf{R}^{\mathrm{SH}})\rho\}$ is the position moment. The trace is over the nuclear (N) degrees of freedom, and ρ is the combined nuclear-electronic density matrix. A derivation of Eq. (16) is available in the supplementary material. Augmented surface hopping stands out as a more rigorous method compared to other approaches because the decoherence rate outside the interaction region is proportional to the force difference, $\mathbf{F}_{jj} - \mathbf{F}_{ii}$, which is fundamentally correct based on an analysis of the quantum-classical Liouville equation.[11] Several other studies (e.g., Refs. 73 and 74) have also derived a decoherence rate that depends on the force difference.

C. DbA model simulations

The DbA model used in our simulations can be rationalized as a linear chain of diatomic molecules, each representing a specific group: donor, bridge, and acceptor [Fig. 2(a)]. The model contains a single bridge state (i.e., $N = 1$), and diabatic potential energy surfaces are parabolic with respect to the reaction coordinate: $E_{DD} = m\omega^2x^2/2 + Mx$, $E_{bb} = m\omega^2(x - x_b)^2/2 + \Delta\epsilon$, and $E_{AA} = m\omega^2x^2/2 - Mx - \epsilon_0$. Here, $M = \sqrt{\lambda m\omega^2/2}$, where λ is the donor-to-acceptor reorganization energy, m is the reduced mass, and ω is the angular frequency. Figure 2(b) shows the adiabatic potential energy surfaces. The bridge diabat is centered at the transition state configuration between a donor and an acceptor at $x_b = -\epsilon_0/2M$, where ϵ_0 is the driving force. The donor-bridge and bridge-acceptor diabatic couplings are relatively weak (i.e., $V_{Db} = V_{bA} = V$) in order to simulate nonadiabatic electron transfer between a donor and an acceptor.

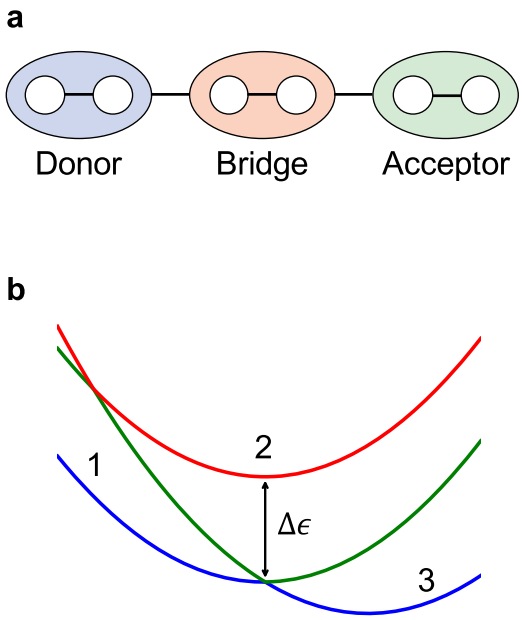

FIG. 2. (a) Cartoon schematic of the DbA model represented as a linear chain of diatomic molecules. (b) Adiabatic potential energy surfaces of the DbA model with respect to the reaction coordinate. Donor, bridge, and acceptor diabats are labeled by 1, 2, and 3, respectively. The tunneling energy gap is labeled by $\Delta\epsilon$.

Trajectories started in the donor diabat with initial positions and momenta sampled from Boltzmann distributions.[75] Each ensemble was made up of 3000 trajectories. Every trajectory evolved with a $\Delta t = 1.25$ a.u. time step for a total of 10^7 time steps. The population of the acceptor diabat was recorded as a function of time and was computed by squaring the inner product of the adiabatic state of the occupied surface with the diabatic state of the acceptor diabat. After averaging over all trajectories, the donor-to-acceptor reaction rate, k, was obtained by fitting the population of the acceptor diabat to the function $1 - \exp(-kt)$. Reaction rates were computed as a function of the driving force (ϵ_0), diabatic coupling (V), and tunneling energy ($\Delta\epsilon$). Constant parameters of the model (in atomic units) are $m = 1$, $\omega = 4.375 \times 10^{-5}$, $\lambda = 2.39 \times 10^{-2}$, $k_B T = 9.50 \times 10^{-4}$, and $\gamma = 1.50 \times 10^{-4}$ (the Langevin friction parameter). These numerical parameters were borrowed from Ref. 30 and are used to simulate reactions on the nanosecond time scale.

V. RESULTS AND DISCUSSION

Figure 3 shows donor-to-acceptor reaction rates. The scaling behavior of the reaction rates were determined with a least-squares

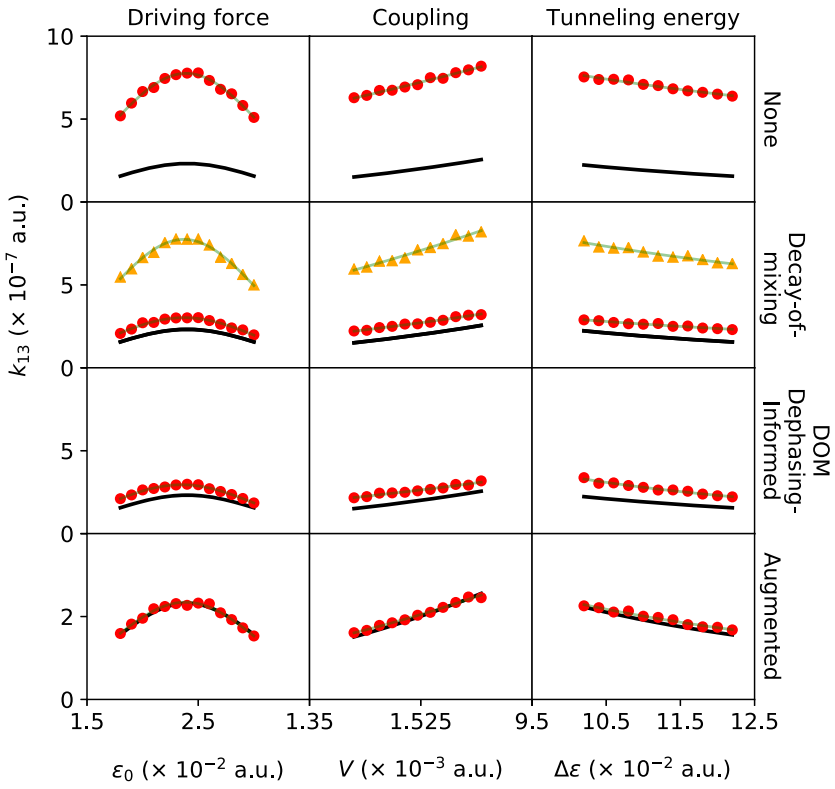

FIG. 3. Donor-to-acceptor reaction rates as a function of driving force (ϵ_0), diabatic coupling (V), and tunneling energy gap ($\Delta\epsilon$). Reaction rates were computed with surface hopping (red circles) and Marcus theory (black lines). Decay-Of-Mixing (DOM) data include $C = 1$ (orange triangles) and $C = 10$ (red circles) [see Eq. (13)]. Curve fits of the surface hopping data are shown in light gray.

fit to Eq. (7). Table I shows fitted parameters of the reorganization energy (λ), scaling in diabatic coupling (V), and scaling in tunneling energy ($\Delta\epsilon$). All methods accurately predict the driving force corresponding to the maximum reaction rate (i.e., when $\epsilon_0 = \lambda$), but the magnitude of the rates as well as scaling behavior varies among the methods. Generally speaking, we find that the donor-to-acceptor reaction rate is related to the frequency of nonadiabatic transitions between the two lowest-energy adiabatic surfaces [Fig. 2(b)]. In the case of a few nonadiabatic events, a trajectory may quickly settle in the acceptor diabat [right of the diabatic crossing in Fig. 2(b)], resulting in a fast reaction rate, k_{13}. Conversely, in the case of many nonadiabatic transitions, the time elapsed before the nuclear coordinate settles in the acceptor diabat will be longer, resulting in a slower k_{13}. The frequency of these nonadiabatic transitions depends on how the electronic density matrix is propagated, with or without decoherence.

GFSH without decoherence significantly overestimates the reaction rates across all tests (Fig. 3) and fails to recover the correct scaling in diabatic coupling and tunneling energy (Table I). In exact quantum dynamics, the coherence between two states increases as the trajectory enters their interaction region and likewise decreases (and eventually decays to zero) as the trajectory leaves their interaction region. Dynamics are compromised when this relation does not hold, especially if the trajectory exits and reenters the

TABLE I. Fitting parameters of the donor-to-acceptor reaction rates of Fig. 3. Data were fit to functions (shown in the column labels) representing the scaling behavior of the Marcus theory expression of Eq. (7) with respect to driving force (ϵ_0), coupling (V), and tunneling energy ($\Delta\epsilon$).

Method	Driving force — $a\exp\left[\frac{(x-b)^2}{c}\right]$	Coupling— ax^b	Tunneling energy— ax^b
None	$b = 2.39 \times 10^{-2}$	$b = 2.00$	$b = -0.97$
Decay-of-mixing ($C = 1$)	2.37×10^{-2}	2.57	−1.04
Decay-of-mixing ($C = 10$)	2.37×10^{-2}	2.92	−1.23
DOM dephasing-informed	2.35×10^{-2}	2.69	−2.18
Augmented (A-GFSH)	2.38×10^{-2}	3.42	−1.71

interaction region; an overcohered electronic density will ultimately give spurious transition probabilities and reaction rates.

Decay-of-mixing is qualitatively correct in that the coherence decays outside the interaction region. However, its decoherence time has adjustable parameters that were originally chosen based on numerical tests (see Ref. 62), which may limit the method's transferability to new systems.[76] In our case, we performed two sets of simulations by adjusting the C parameter of the decoherence time [Eq. (13)] and found that the magnitude of the reaction rate is very sensitive to this change; the reaction rate decreased by approximately three-fold from $C = 1$ to $C = 10$ (Fig. 3). The $C = 10$ reaction rates are in very good agreement with Marcus theory based on their magnitude as well as scaling in coupling and tunneling energy (Table I), but this choice of C was chosen by mere trial-and-error. Therefore, the method's applicability to other systems might be open to serious challenge without further reparameterization.

On the basis of the results of Fig. 3 and Table I, the best performing methods are decay-of-mixing dephasing-informed and augmented surface hopping. Each method has notable advantages that make it appealing. In the case of augmented surface hopping, the decoherence rate is relatively rigorous in its formulation and explicitly depends on the force difference between the two decohering potential energy surfaces. This property proves to be important for recovering Marcus theory with the best quantitative accuracy. Moreover, the decoherence rate does not contain any predefined parameters and is presumed to be applicable to various types of systems, although further testing is needed to validate this claim. In the case of decay-of-mixing dephasing-informed, the decoherence rate is more general than that of the original decay-of-mixing method since it contains information specific to the system under consideration. As a result, the magnitude of the method's reaction rates is in much better agreement to Marcus theory (e.g., compare $C = 1$ results to decay-of-mixing dephasing-informed in Fig. 3). Also noteworthy is that reparameterization of the decoherence rate via the dephasing function obeys the correct limiting behavior in which wavepackets on parallel surfaces do not decohere. However, a potential downside to the dephasing-informed approach is the necessity of an accurate and sufficient sampling of the potential energy surfaces involved during the dynamics to calculate the dephasing function [Eq. (15a)]. For the case shown here, we were dealing with a one-dimensional model in which these criteria were easy to adhere to.

VI. SUMMARY AND CONCLUSIONS

Electronic state mixing in a Born-Oppenheimer nuclear-electronic system is controlled by the overlap of nuclear wavepackets on different potential energy surfaces. Dissimilar forces on potential energy surfaces cause the overlap of nuclear wavepackets to diminish, leading to decoherence. Due to classical and independent nuclear trajectories in surface hopping, the electronic density matrix is integrated with fictitious coherence between states that severely compromise transition probabilities. The evolution of the electronic density matrix must be corrected such that it continuously decoheres outside the interaction region. Herein, popular ad hoc and practical first-principles approaches that incorporate decoherence into the evolution of the electronic density matrix were assessed by comparing their donor-to-acceptor reaction rates to Marcus theory.

The strengths and weaknesses of the decoherence methods were evaluated in the context of a Donor-bridge-Acceptor (DbA) model. Truhlar's decay-of-mixing decoheres the electronic density matrix outside the interaction region and qualitatively agrees with Marcus theory. However, we find that the quality of decay-of-mixing depends on predefined parameters; it was only by trial-and-error that the chosen parameters gave reasonable results. We further introduced a method that alleviates this issue by showing that the decoherence rate can be parameterized for the system under investigation as long as an accurate and sufficient sampling of the potential energy surfaces involved in the dynamics is attainable. The method, which we call decay-of-mixing dephasing-informed, is in very good agreement with Marcus theory. Finally, the decoherence rate between electronic states in Subotnik's augmented surface hopping explicitly depends on the force difference between their surfaces. This feature proves to be important for recovering both the magnitude of the reaction rates and the correct scaling in diabatic coupling and tunneling energy with quantitative accuracy.

On the basis of our benchmark study, the decoherence method used to correct surface hopping simulations must be chosen with great care. Our tests of popular methods indicate their broadly varying system-dependent performance. Thus, it is recommended that the method of choice be justified for the system under investigation. Further testing such as higher dimensional potential energy surfaces and a broader range of reaction time scales would provide deeper insight into the advantages and disadvantages of the methods discussed in this paper. For example, a follow-up study comparing decay-of-mixing dephasing-informed and augmented surface hopping would be especially interesting since they were the most successful methods for the DbA model. Information regarding their versatility to new systems and numerical costs may help to clarify their realm of applicability.

SUPPLEMENTARY MATERIAL

See supplementary material for derivation of augmented surface hopping decoherence rate and numerical tests of A-GFSH using two- and three-level scattering models.

ACKNOWLEDGMENTS

We thank Professor Subotnik for the exact solutions of model X in the supplementary material. This work was supported by the U.S. National Science Foundation, Grant No. CHE-1900510. L.W. acknowledges support from the National Natural Science Foundation of China (Grant Nos. 21873080 and 21703202). Computational resources were supported by the University of Southern California's Center for High-Performance Computing. This work was done in part at the Center for Nonlinear Studies (CNLS) at Los Alamos National Laboratory and the Center for Integrated Nanotechnologies (CINT), a U.S. Department of Energy and Office of Basic Energy Sciences user facility. A.E.S. thanks CNLS for their support and hospitality.

REFERENCES

[1] J. Tully, J. Chem. Phys. **93**, 1061 (1990).
[2] S. Hammes-Schiffer and J. C. Tully, J. Chem. Phys. **101**, 4657 (1994).
[3] U. Müller and G. Stock, J. Chem. Phys. **107**, 6230 (1997).
[4] J. C. Tully, Annu. Rev. Phys. Chem. **51**, 153 (2000).
[5] S. Hammes-Schiffer, Acc. Chem. Res. **34**, 273 (2001).
[6] T. Nelson, S. Fernandez-Alberti, V. Chernyak, A. E. Roitberg, and S. Tretiak, J. Phys. Chem. B **115**, 5402 (2011).
[7] A. V. Akimov, A. J. Neukirch, and O. V. Prezhdo, Chem. Rev. **113**, 4496 (2013).
[8] T. Nelson, S. Fernandez-Alberti, A. E. Roitberg, and S. Tretiak, Acc. Chem. Res. **47**, 1155 (2014).
[9] L. J. Wang, O. V. Prezhdo, and D. Beljonne, Phys. Chem. Chem. Phys. **17**, 12395 (2015).
[10] R. Long, O. V. Prezhdo, and W. Fang, Wiley Interdiscip. Rev.: Comput. Mol. Sci. **7**, e1305 (2017).
[11] J. E. Subotnik, A. Jain, B. Landry, A. Petit, W. Ouyang, and N. Bellonzi, Annu. Rev. Phys. Chem. **67**, 387 (2016).
[12] J.-Y. Fang and S. Hammes-Schiffer, J. Phys. Chem. A **103**, 9399 (1999).
[13] J. E. Subotnik, J. Phys. Chem. A **115**, 12083 (2011).
[14] S. V. Kilina, D. S. Kilin, and O. V. Prezhdo, ACS Nano **3**, 93 (2008).
[15] B. F. Habenicht, C. F. Craig, and O. V. Prezhdo, Phys. Rev. Lett. **96**, 187401 (2006).
[16] S. V. Kilina, A. J. Neukirch, B. F. Habenicht, D. S. Kilin, and O. V. Prezhdo, Phys. Rev. Lett. **110**, 180404 (2013).
[17] B. F. Habenicht and O. V. Prezhdo, Phys. Rev. Lett. **100**, 197402 (2008).
[18] J. Xu and L. Wang, J. Chem. Phys. **150**, 164101 (2019).
[19] X. Gao and W. Thiel, Phys. Rev. E **95**, 013308 (2017).
[20] H. M. Jaeger, S. Fischer, and O. V. Prezhdo, J. Chem. Phys. **137**, 22A545 (2012).
[21] J. E. Subotnik and N. Shenvi, J. Chem. Phys. **134**, 024105 (2011).
[22] N. Shenvi, J. E. Subotnik, and W. Yang, J. Chem. Phys. **134**, 144102 (2011).
[23] G. Granucci, M. Persico, and A. Zoccante, J. Chem. Phys. **133**, 134111 (2010).
[24] R. E. Larsen, M. J. Bedard-Hearn, and B. J. Schwartz, J. Phys. Chem. B **110**, 20055 (2006).
[25] M. J. Bedard-Hearn, R. E. Larsen, and B. J. Schwartz, J. Chem. Phys. **123**, 234106 (2005).
[26] E. R. Bittner and P. J. Rossky, J. Chem. Phys. **103**, 8130 (1995).
[27] B. R. Landry and J. E. Subotnik, J. Chem. Phys. **135**, 191101 (2011).
[28] E. Neria and A. Nitzan, J. Chem. Phys. **99**, 1109 (1993).
[29] C. A. Schwerdtfeger, A. V. Soudackov, and S. Hammes-Schiffer, J. Chem. Phys. **140**, 034113 (2014).
[30] B. R. Landry and J. E. Subotnik, J. Chem. Phys. **137**, 22A513 (2012).
[31] H.-T. Chen and D. R. Reichman, J. Chem. Phys. **144**, 094104 (2016).
[32] O. S. Wenger, Acc. Chem. Res. **44**, 25 (2011).
[33] J. Jortner, M. Bixon, T. Langenbacher, and M. E. Michel-Beyerle, Proc. Natl. Acad. Sci. U. S. A. **95**, 12759 (1998).
[34] Y. Hu and S. Mukamel, Chem. Phys. Lett. **160**, 410 (1989).
[35] H. M. McConnell, J. Chem. Phys. **35**, 508 (1961).
[36] F. D. Lewis, J. Liu, W. Weigel, W. Rettig, I. V. Kurnikov, and D. N. Beratan, Proc. Natl. Acad. Sci. U. S. A. **99**, 12536 (2002).
[37] F. D. Lewis, T. Wu, X. Liu, R. L. Letsinger, S. R. Greenfield, S. E. Miller, and M. R. Wasielewski, J. Am. Chem. Soc. **122**, 2889 (2000).
[38] D. Hanss and O. S. Wenger, Inorg. Chem. **48**, 671 (2008).
[39] D. Hanss and O. S. Wenger, Inorg. Chem. **47**, 9081 (2008).
[40] G. L. Closs and J. R. Miller, Science **240**, 440 (1988).
[41] P. P. Edwards, H. B. Gray, M. T. Lodge, and R. J. Williams, Angew. Chem., Int. Ed. **47**, 6758 (2008).
[42] B. Albinsson, M. P. Eng, K. Pettersson, and M. U. Winters, Phys. Chem. Chem. Phys. **9**, 5847 (2007).
[43] H. B. Gray and J. R. Winkler, Proc. Natl. Acad. Sci. U. S. A. **102**, 3534 (2005).
[44] E. A. Badaeva, T. V. Timofeeva, A. Masunov, and S. Tretiak, J. Phys. Chem. A **109**, 7276 (2005).
[45] A. E. Sifain, L. F. Tadesse, J. A. Bjorgaard, D. E. Chavez, O. V. Prezhdo, R. J. Scharff, and S. Tretiak, J. Chem. Phys. **146**, 114308 (2017).
[46] L. J. Wang, D. Trivedi, and O. V. Prezhdo, J. Chem. Theory Comput. **10**, 3598 (2014).
[47] A. E. Sifain, L. J. Wang, and O. V. Prezhdo, J. Chem. Phys. **142**, 224102 (2015).
[48] D. G. Truhlar, *Quantum Dynamics of Complex Molecular Systems* (Springer, 2007), pp. 227–243.
[49] A. Nitzan, *Chemical Dynamics in Condensed Phases: Relaxation, Transfer and Reactions in Condensed Molecular Systems* (Oxford University Press, 2006).
[50] J.-Y. Fang and S. Hammes-Schiffer, J. Chem. Phys. **110**, 11166 (1999).
[51] J. Spencer, L. Scalfi, A. Carof, and J. Blumberger, Faraday Discuss. **195**, 215 (2016).
[52] J. Peng, Y. Xie, D. Hu, and Z. Lan, J. Chem. Phys. **150**, 164126 (2019).
[53] A. A. Kananenka, X. Sun, A. Schubert, B. D. Dunietz, and E. Geva, J. Chem. Phys. **148**, 102304 (2018).
[54] M. Born and K. Huang, *Dynamical Theory of Crystal Lattices* (Clarendon Press, 1954).
[55] O. V. Prezhdo and P. J. Rossky, Phys. Rev. Lett. **81**, 5294 (1998).
[56] L. J. Wang, A. E. Sifain, and O. V. Prezhdo, J. Phys. Chem. Lett. **6**, 3827 (2015).
[57] L. J. Wang, A. E. Sifain, and O. V. Prezhdo, J. Chem. Phys. **143**, 191102 (2015).
[58] Conventional FSSH is unable to describe the transfer invoking superexchange-like pathways in the diabatic representation. GFSH was developed to circumvent this deficiency.[46]
[59] A. Jain and J. E. Subotnik, J. Chem. Phys. **143**, 134107 (2015).
[60] A. E. Sifain, L. Wang, and O. V. Prezhdo, J. Chem. Phys. **144**, 211102 (2016).
[61] S. C. Cheng, C. Zhu, K. K. Liang, S. H. Lin, and D. G. Truhlar, J. Chem. Phys. **129**, 024112 (2008).
[62] C. Zhu, S. Nangia, A. W. Jasper, and D. G. Truhlar, J. Chem. Phys. **121**, 7658 (2004).
[63] O. V. Prezhdo, J. Chem. Phys. **111**, 8366 (1999).
[64] A. V. Akimov and O. V. Prezhdo, J. Phys. Chem. Lett. **4**, 3857 (2013).
[65] S. Mukamel, *Principles of Nonlinear Optical Spectroscopy* (Oxford University Press, New York, 1995), Vol. 29.
[66] R. Long, W. Fang, and A. V. Akimov, J. Phys. Chem. Lett. **7**, 653 (2016).
[67] Z. Zhang, R. Long, M. V. Tokina, and O. V. Prezhdo, J. Am. Chem. Soc. **139**, 17327 (2017).
[68] J. He, A. S. Vasenko, R. Long, and O. V. Prezhdo, J. Phys. Chem. Lett. **9**, 1872 (2018).
[69] Z. Zhang, W.-H. Fang, M. V. Tokina, R. Long, and O. V. Prezhdo, Nano Lett. **18**, 2459 (2018).
[70] Here, we make the assumption that the classical path approximation (CPA) is valid. CPA assumes that ground state trajectories sample nuclear geometries that are seen during excited state dynamics. For example, CPA is valid for systems in which forces on the ground and excited states are similar.
[71] A. V. Akimov and O. V. Prezhdo, J. Chem. Theory Comput. **9**, 4959 (2013).
[72] Similar Gaussian behavior can be seen by taking the classical limit of the dephasing function for the two displaced harmonic oscillator problem of Marcus theory.
[73] B. J. Schwartz, E. R. Bittner, O. V. Prezhdo, and P. J. Rossky, J. Chem. Phys. **104**, 5942 (1996).
[74] O. V. Prezhdo and P. J. Rossky, J. Chem. Phys. **107**, 5863 (1997).
[75] For each trajectory, position and momentum were sampled from Gaussian distributions with mean (μ) and standard deviation (σ) given by $\{\mu,\sigma\} = \{-M/m\omega^2, \sqrt{k_B T/m\omega^2}\}$ and $\{0, \sqrt{mk_B T}\}$, respectively.
[76] T. Nelson, S. Fernandez-Alberti, A. E. Roitberg, and S. Tretiak, J. Chem. Phys. **138**, 224111 (2013).